

RESEARCH ARTICLE

Insights on stream temperature processes through development of a coupled hydrologic and stream temperature model for forested coastal headwater catchments

Jason A. Leach¹  | Dan Moore²

¹Department of Geography, Simon Fraser University, 8888 University Drive Burnaby, British Columbia, Canada

²Department of Geography, University of British Columbia, 1984 West Mall, Vancouver, British Columbia, Canada

Correspondence

Jason A. Leach, Department of Geography, Simon Fraser University, 8888 University Drive, Burnaby, British Columbia, Canada.

Email: jleach@sfu.ca

Abstract

Stream temperature controls a number of biological, chemical, and physical processes occurring in aquatic environments. Transient snow cover and advection associated with lateral throughflow inputs can have a dominant influence on stream thermal regimes for headwater catchments in the rain-on-snow zone. Most existing stream temperature models lack the ability to properly simulate these processes. We developed and evaluated a conceptual-parametric catchment-scale stream temperature model that includes the role of transient snow cover and lateral advection associated with throughflow. The model consists of routines for simulating canopy interception, snow accumulation and melt, hillslope throughflow runoff and temperature, and stream channel energy exchange processes. The model was used to predict discharge and stream temperature for a small forested headwater catchment near Vancouver, Canada, using long-term (1963–2013) weather data to compute model forcing variables. The model was evaluated against 4 years of observed stream temperature. The model generally predicted daily mean stream temperature accurately (annual RMSE between 0.57 and 1.24 °C) although it overpredicted daily summer stream temperatures by up to 3 °C during extended low streamflow conditions. Model development and testing provided insights on the roles of advection associated with lateral throughflow, channel interception of snow, and surface–subsurface water interactions on stream thermal regimes. This study shows that a relatively simple but process-based model can provide reasonable stream temperature predictions for forested headwater catchments located in the rain-on-snow zone.

KEYWORDS

channel interception, headwater, rain-on-snow, stream temperature, throughflow, winter thermal regime

1 | INTRODUCTION

Stream temperature influences a variety of aquatic ecosystem processes, such as dissolved oxygen concentrations, macroinvertebrate emergence timing, and fish distribution, survival, and growth (Lee & Rinne, 1980; Beacham & Murray, 1990; Ebersole, Liss, & Frissell, 2001; Harper & Peckarsky, 2006; Leach, Moore, Hinch, & Gomi, 2012). Land cover and climatic changes can alter stream thermal regimes, which in turn impact aquatic ecosystems (Moore, Spittlehouse, & Story, 2005a; Durance & Ormerod, 2007; Isaak, Wollrab, Horan, & Chandler, 2012; Penaluna et al., 2015). To effectively manage and sustain healthy aquatic environments, we need better predictive tools that will depend upon an improved understanding of the processes controlling stream temperature and their response to environmental change (Webb,

Hannah, Moore, Brown, & Nobilis, 2008; Arismendi, Johnson, Dunham, & Haggerty, 2013; Lisi, Schindler, Cline, Scheuerell, & Walsh, 2015).

Most process-based predictive stream temperature models are focused on accurately representing the energy fluxes occurring at the stream-air interface, and less emphasis is placed on advective fluxes associated with groundwater, hyporheic, and runoff processes (Theurer, Voos, & Miller, 1984; Boyd & Casper, 2003). This focus likely reflects that most process-based stream temperature research has focused on summer periods, usually within the context of summer maximum temperatures and associated upper thermal tolerances of fish and other aquatic organisms (Eaton & Scheller, 1996; Wehrly, Wang, & Mitro, 2007; Isaak et al., 2016). Energy exchanges at the atmosphere and stream surface interface, particularly net radiation, are often the dominant control on summer stream temperature patterns

(Brown, 1969; Moore, Sutherland, Gomi, & Dhakal, 2005b; Hannah, Malcolm, Soulsby, & Youngson, 2008; Leach & Moore, 2010; Garner, Malcolm, Sadler, Millar, & Hannah, 2015). However, in some reaches, groundwater–surface water interactions can significantly moderate temperature variability (Story, Moore, & Macdonald, 2003; Johnson, 2004; Leach & Moore, 2011; MacDonald, Boon, Byrne, & Silins, 2014b; Wagner et al., 2014). Only recently have these hydrologic processes been given more attention in the development of predictive stream temperature models (e.g., Comola, Schaeffli, Rinaldo, & Lehning, 2015; Kurylyk, MacQuarrie, Caissie, & McKenzie, 2015; Gallice et al., 2016).

Winter stream thermal regimes have received less attention than summer regimes despite the known importance of winter periods for aquatic ecosystems (Beschta, Bilby, Brown, Holtby, & Hofstra, 1987; Holtby, 1988; Ebersole et al., 2006; Brown, Hubert, & Daly, 2011; Shuter, Finstad, Helland, Zweimüller, & Höller, 2012). Empirical research has suggested that winter and summer periods are characterized by distinct thermal regimes, reflecting seasonal differences in the dominant energy exchange processes (Webb & Zhang, 1999; Malard, Mangin, Uehlinger, & Ward, 2001; Danehy, Colson, & Duke, 2010; Arismendi et al., 2013). Headwater catchments in temperate regions, such as the coastal portion of the Pacific Northwest, experience moderate air temperatures and, depending on the elevation zone, infrequent, transient, or seasonally continuous snow cover. The winter hydrologic regime is dominated by throughflow, hillslope soil water that flows laterally downslope before entering the stream, associated with rain and rain-on-snow events. Headwater streams in these regions typically remain unfrozen during most of the winter, and transient snow cover and lateral advection associated with hillslope runoff processes are important influences on winter thermal regime (Leach & Moore, 2014).

We previously evaluated the ability of existing stream temperature models to estimate throughflow temperature, as well as their ability to represent the role of transient snow cover on throughflow temperature (Leach & Moore, 2015). Two primary issues with current catchment-scale predictive stream temperature models were highlighted that limit their ability to properly simulate winter stream thermal conditions at headwater catchments in the rain-on-snow zone: (a) most models cannot account for the role of transient snow cover on the temperature of lateral throughflow and (b) models that do account for transient snow cover inaccurately estimate the temperature of lateral throughflow by up to 5 °C. In addition, most models specify the upstream temperature boundary condition using observations or empirical relations with air temperature (e.g., MacDonald, Boon, & Byrne, 2014a; Sun, Yearsley, Voisin, & Lettenmaier, 2015), which limits their usefulness as predictive tools. Recent stream temperature model developments have further highlighted the importance of advective inputs associated with subsurface water on the thermal regimes of small- and meso-scale catchments (Comola et al., 2015; Gallice et al., 2016).

The overall objective of this study was to develop and evaluate a conceptual-parametric catchment-scale stream temperature model that included the role of transient snow cover and lateral advection associated with throughflow. Rigorous model testing using detailed field observations can be used to develop a better understanding of hydrologic processes governing stream temperature to ensure that we are getting correct predictions for the right reasons

(*sensu* Kirchner, 2006). In this study, insights on the roles of advection associated with lateral throughflow, channel interception of snow, and surface–subsurface water interactions on stream temperature were gained during the model development and testing phases.

2 | STUDY AREA

2.1 | Malcolm knapp research forest

This study was conducted at the University of British Columbia's Malcolm Knapp Research Forest (MKRF), located at 49° 16' N and 122° 34' W, about 60 km east of Vancouver (Figure 1). The area experiences a maritime climate with wet mild winters and warm dry summers. Mean annual precipitation at the Environment Canada climate station located at the research forest headquarters (Haney UBC RF Admin, station number 1103332), elevation 147 m above sea level (asl), is 2184 mm, of which 70% falls primarily as rain between October and April due to Pacific frontal systems. Snowfall comprises only 5% of the total annual precipitation at the low elevation headquarters but increases at higher elevations. Based on data from 1962 to 2013, mean annual air temperature is 9.6 °C and mean monthly temperatures for January and July during this period are 2.4 and 17.3 °C, respectively.

Most of MKRF lies in the Coastal Western Hemlock biogeoclimatic zone, with the highest elevation bands lying in the Mountain Hemlock zone (Krajina, 1965). MKRF has experienced considerable harvesting and forest disturbance over the last century and therefore comprises a patchwork of variable forest stand compositions and ages, dominated by second growth western red cedar (*Thuja plicata*), Douglas-fir (*Pseudotsuga menziesii*), and western hemlock (*Tsuga heterophylla*).

Soils are primarily coarse-textured humo-ferric podzols (Feller & Kimmins, 1979). Soil depths range up to 2 m, with compacted till or granitic bedrock found on average at 1-m depth. Bedrock outcrops occur in places, especially along topographic divides. Average hydraulic conductivities are typically 10^{-4} to 10^{-3} m s $^{-1}$ in the soil and 10^{-7} to 10^{-6} m s $^{-1}$ in the underlying till (Utting, 1979; Cheng, 1988). Partially as a result of tree-throw, the forest floor has a complex topography, with marked changes in convexity/concavity over distances of 2–5 m.

Owing to the high permeability of the soils, almost all water reaching the ground surface infiltrates the soil and flows downslope in a saturated layer above the contact between the soil and underlying till or bedrock. Streamflow typically responds rapidly to rainfall. Runoff generation processes are dominated by subsurface flow and, to a lesser extent, saturation-excess overland flow (Thompson & Moore, 1996; Donnelly-Makovecki & Moore, 1999; Hutchinson & Moore, 2000; Haught & van Meerveld, 2011). Most stormflow occurs in the autumn-winter wet season and many streams dry up during the summer.

2.2 | Griffith and east creeks

The study focused on two headwater catchments within MKRF: Griffith Creek and East Creek. At the location of a weir for stream gauging, Griffith Creek's catchment ranges from 370 to 570 m asl and has a catchment area of 11 ha. Griffith Creek has been intensively

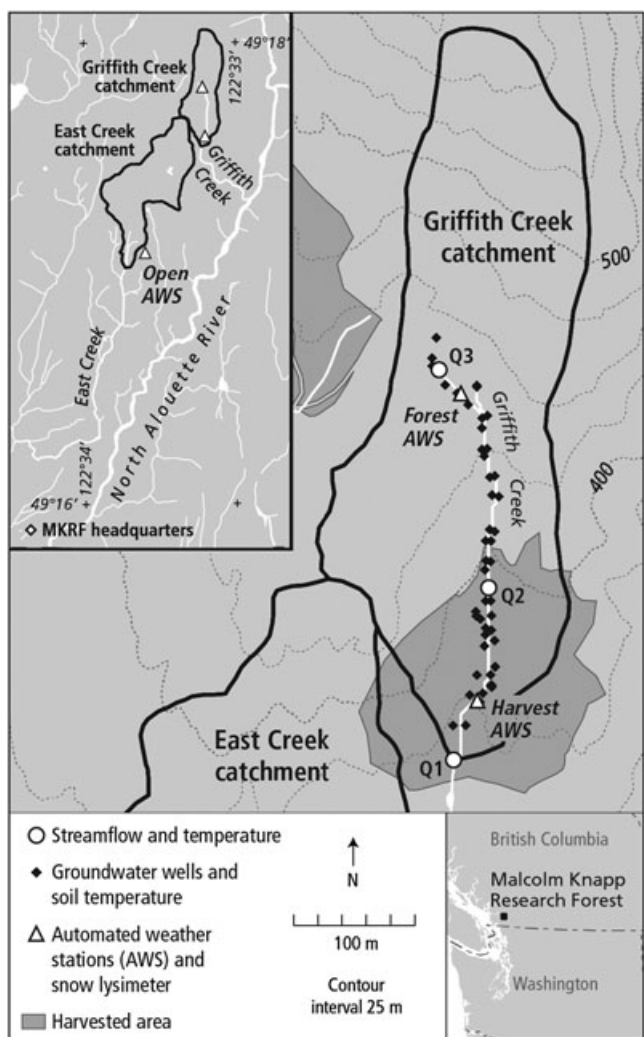


FIGURE 1 Map of the Malcolm Knapp Research Forest showing (a) map of Griffith Creek where most of the detailed field measurements that informed the model development were made and (b) an inset showing Griffith and East creeks, open site meteorological station, and the MKRF headquarters (location of the Environment Canada meteorological station)

monitored for various hydrometric, microclimate, and stream temperature measurements during both summer (Guenther, 2007; Guenther, Gomi, & Moore, 2014) and winter periods (Leach & Moore, 2014). The findings and data collected from these studies were used to conceptualize and help calibrate the stream temperature model presented here. Field data relevant to this study are described in the following section. Additional details and background on the instrumentation and measurements made at Griffith Creek can be found in Guenther, Moore, and Gomi (2012), Guenther et al., (2014), and Leach and Moore (2014, 2015).

Whereas data collected at Griffith Creek were used to inform and develop the stream temperature model, the model was applied and evaluated against observations from East Creek. At the location of a weir, East Creek's catchment ranges from 290 to 440 m asl, with a drainage area of 38 ha. East Creek was used to test the model primarily for three reasons: (a) East Creek provides an independent evaluation test because the hillslope throughflow temperature component of the

stream temperature model was calibrated for Griffith Creek (Leach & Moore, 2015); (b) East Creek has a relatively long period of monitoring at the outlet for both streamflow (1972 to 2013 with extended gaps) and stream temperature (1997 to 2003, 2008, and 2010 to 2013), in comparison to other headwater catchments in MKRF; and (c) East Creek supports a population of resident cutthroat trout (*Oncorhynchus clarki clarki*), thereby adding biological relevance to the stream temperature modelling (Boss and Richardson, 2002; Leach et al., 2012).

3 | DATA COLLECTION AND PROCESSING

3.1 | Meteorological stations

Four meteorological stations were used in this study to generate hourly air temperature and precipitation used as input to the stream temperature model. The Environment Canada long-term climate station (147-m elevation) reports daily total precipitation and daily maximum and minimum air temperature (data used in this study are from 1962 to 2013). Three additional meteorological stations installed at MKRF (Guenther et al., 2012; Leach & Moore, 2014) were used to record air temperature at 10-min intervals, from which hourly means were computed: (a) East Creek open station (operated from July 2003 to November 2006, and from July 2011 to May 2013; 300-m elevation), (b) Griffith Creek forest station (operated July 2011 to May 2013; 440-m elevation), and (c) East Creek forest station (operated October 2012 to May 2013; 295-m elevation). A summary of all data collected for the study and how they were used for the stream temperature modelling is provided in Figure 2.

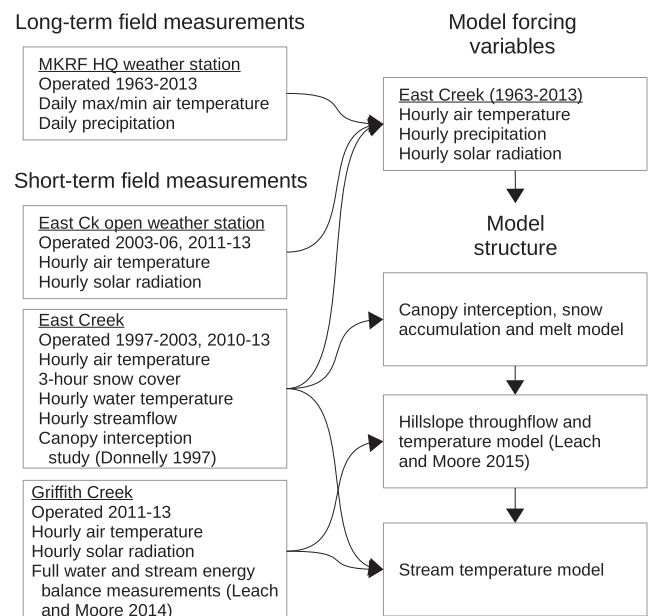


FIGURE 2 Overview of the field measurements and modelling chain highlighting the long-term field measurements from the MKRF HQ Environment Canada weather station, the short-term (2 years or less) field measurements from East and Griffith creeks, the model forcing variables, and the model structure components. Arrows indicate where specific field measurements were used in the model development and testing

3.2 | East Creek discharge, stream temperature, and snow cover

East Creek was outfitted with a weir and stage level recorder to monitor streamflow. East Creek also had submersible temperature sensor loggers installed at the outlet recording at 15-min intervals. For the 2012–2013 winter, air temperature and relative humidity sensors (HOBO Pro v2 U23, Onset Computer Corporation, Bourne, MA) were installed above East Creek to characterize above-stream microclimate. In addition, a time-lapse camera was installed at East Creek during 2011–2013 to determine periods of snow cover. These data were used to calibrate and evaluate internal routines within the coupled hydrologic and stream temperature model.

3.3 | Generation of hourly precipitation and air temperature

Daily precipitation from the Environment Canada station was adjusted for differences in elevation between the Environment Canada climate station and East Creek by multiplying by 1.16 (Donnelly-Makovecki & Moore, 1999), and daily values were divided by 24 in order to downscale to hourly values. Missing daily precipitation values were set to zero. Based on water balance calculations comparing annual precipitation, estimated evapotranspiration and discharge totals, the precipitation multiplier of 1.16 was insufficient to produce the amount of water leaving the East Creek catchment calculated from discharge at the weir. Errors in the precipitation multiplier, catchment area delineation, and stage-discharge rating curve are possibilities for the water balance discrepancy. We address these uncertainties in more detail in the discussion. To explore the sensitivity of the stream temperature predictions to uncertainties in the water balance, we also ran the model using a precipitation correction factor of 2.0, which resulted in better closure of the annual water balance, and compared the resulting stream temperature predictions with observations and predictions made using a 1.16 correction factor.

Hourly air temperatures for below canopy conditions at East Creek were interpolated from daily minimum and maximum air temperature measured at the Environment Canada station. These air temperatures were corrected for both elevation differences between the MKRF headquarters and East Creek, as well as differences between open site and below canopy conditions. This was accomplished using the three additional meteorological stations described above. To adjust for differences between open site and below canopy conditions, monthly median differences between open site and below canopy air temperatures, d_k , for month k were computed as

$$d_k = \hat{T}_{GCO,k} - T_{GCF,k}, \quad (1)$$

where $T_{GCF,k}$ is monthly median of daily maximum or minimum air temperature from the Griffith Creek below canopy forest station, and $\hat{T}_{GCO,k}$ is monthly median of predicted daily maximum or minimum air temperature from the East Creek open station after adjusting for the elevation difference between East Creek open and Griffith Creek forest weather stations as follows:

$$\hat{T}_{GCO,j} = T_{ECO,j} - \gamma(z_{GCF} - z_{ECO}), \quad (2)$$

where $T_{ECO,j}$ is daily maximum or minimum air temperatures from the East Creek open station, γ is a standard temperature lapse rate ($0.006^{\circ}\text{C m}^{-1}$), and z_{GCF} and z_{ECO} are elevations (m) of the Griffith Creek forest and East Creek open weather stations, respectively.

Daily maximum or minimum air temperatures observed at the Environment Canada climate station, $T_{HQ,j}$ ($^{\circ}\text{C}$), on day j were adjusted to the elevation of East Creek:

$$\hat{T}_{ECO,j} = T_{HQ,j} - \gamma(z_{ECF} - z_{HQ}), \quad (3)$$

where $\hat{T}_{ECO,j}$ is predicted daily maximum or minimum open air temperature for the East Creek elevation, and z_{ECF} and z_{HQ} are the elevations, in m, of the East Creek forest station and Environment Canada MKRF headquarter climate stations, respectively.

Daily maximum or minimum air temperature below the forest canopy at East Creek, $T_{ECF,j}$ ($^{\circ}\text{C}$), on day j was calculated as

$$\hat{T}_{ECF,j} = \hat{T}_{ECO,j} + d_k, \quad (4)$$

where d_k corrects for forest and open site differences by month.

Hourly air temperatures were generated from the daily maximum and minimum air temperatures estimated for the East Creek forest site ($\hat{T}_{ECF,j}$) by interpolating between daily maximum and minimum values using the following:

$$T_{pred}(t) = \begin{cases} T_1 + (T_2 - T_1) \cdot 0.5(1 + \cos(\pi + \pi \lambda_t / \Delta t)), & T_2 \geq T_1 \\ T_1 + (T_2 - T_1) \cdot 0.5(1 + \cos(\pi + \pi \lambda_t / \Delta t))^{0.5}, & T_1 > T_2 \end{cases}, \quad (5)$$

where $T_{pred}(t)$ is the predicted air temperature for hour t , T_1 is either the daily maximum or minimum air temperature, T_2 is the daily maximum or minimum air temperature after T_1 (all in $^{\circ}\text{C}$), λ_t is the hour following T_1 , and Δt is the number of hours between T_1 and T_2 . The hour that T_1 and T_2 occurred on a given day was determined by calculating median times of daily maximum and minimum air temperatures by month from the East Creek open station. The predicted air temperature was evaluated against observed hourly air temperature measured at the East Creek forest station during October 2012 to May 2013.

3.4 | Estimation of solar radiation

Solar radiation reaching the stream surface was estimated by first computing daily incoming solar radiation following approaches of Bristow and Campbell (1984) and Thornton and Running (1999):

$$K \downarrow = \tau_t \cdot K_{max}, \quad (6)$$

where $K \downarrow$ is daily total global horizontal radiation ($\text{MJ m}^{-2} \text{ day}^{-1}$); τ_t is daily total transmissivity (unitless); and K_{max} is daily total potential radiation ($\text{MJ m}^{-2} \text{ day}^{-1}$) calculated using approaches of Iqbal (1983) and Kasten and Young (1989). The daily total transmissivity was calculated as

$$\tau_t = A[1 - \exp(-B \cdot \Delta T^C)], \quad (7)$$

where A , B , and C are empirical coefficients, and ΔT is the diurnal range in air temperature taken from the Environment Canada meteorological station. The coefficients A , B , and C were estimated using nonlinear least squares regression using ΔT for the period of 2003 to 2006 from the Environment Canada meteorological station and τ_t calculated from K_{max} and observed $K \downarrow$ from an open meteorological station near East Creek that was operational from 2003 to 2006 (Guenther, 2007).

For each day, j , values of K_{\downarrow} were computed for each minute, i , as follows:

$$K_{\downarrow,i,j} = \begin{cases} \frac{\cos\theta_{i,j}}{\sum\limits_{i=1}^{1440} \cos\theta_{i,j} \delta_{i,j}} \cdot K_{\downarrow,j}, & \cos\theta_{i,j} > 0 \\ 0, & \cos\theta_{i,j} \leq 0 \end{cases}, \quad (8)$$

where $\theta_{i,j}$ is the solar zenith angle for minute i on day j , and $\delta_{i,j}$ equals one if $\cos\theta_{i,j} > 0$ and 0 otherwise and restricts the calculation to periods when the sun is above the horizon. Hourly values of K_{\downarrow} were then computed by averaging the 1-min values for each hour of the day. We assumed that 5% of above-canopy K_{\downarrow} reached the stream surface (Guenther, 2007). Predicted hourly K_{\downarrow} was compared to measured K_{\downarrow} from a Griffith Creek forest meteorological station for the 2011 to 2013 period.

4 | MODEL DESCRIPTION, CALIBRATION, AND TESTING

4.1 | Model description

The stream temperature model extends a hillslope throughflow temperature model (Leach & Moore, 2015) by adding canopy interception, snow accumulation and melt, and stream channel water and heat balance calculations (Figure 3). The model is spatially lumped and can output simulated snow pack dynamics, stream discharge, and temperature at subdaily time intervals. A detailed description of the model structure and governing equations are provided in the appendix and a list of model parameters are shown in Table 1. A key component of the model is the throughflow temperature routine detailed in Leach and Moore (2015). The throughflow temperature routine consists of upslope and downslope hillslope reservoirs, and throughflow and thermal dynamics are simulated using simplified representations of hydrologic and thermal processes. See Leach and Moore (2015) for details of the throughflow model and its calibration. The following section describes the calibration and testing of the coupled hydrologic and stream temperature model.

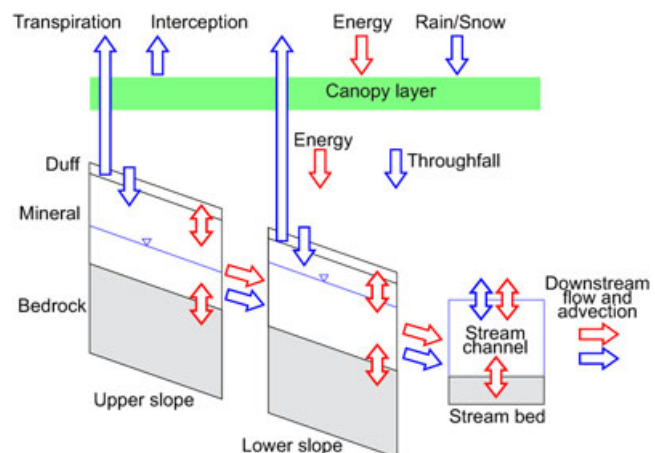


FIGURE 3 Schematic diagram of the stream temperature model including the canopy interception, hillslope throughflow, and stream channel components. Blue arrows represent water fluxes and red arrows represent energy fluxes between the various model components

4.2 | Calibration and testing

The full stream temperature model described in the appendix incorporates and adapts two previously developed model routines: the canopy interception model from Donnelly-Makovecki and Moore (1999) and the hillslope throughflow temperature model from Leach and Moore (2015), both of which were developed using field data collected at MKRF. Most of the parameters that require calibration in these model components were set to the calibrated values reported in these two studies. Exceptions include the snow canopy interception efficiency and canopy snow storage capacity, which used results from Martin et al. (2013), and adjustment of the hillslope throughflow model to account for differences in catchment characteristics between Griffith and East creeks. These latter adjustments include setting the mean hillslope angle to 10.6° (parameter ζ in Leach and Moore, 2015) determined from a 5m digital elevation model, and a reach length of 1100m. In addition, the temperature at the depth below the surface where it is assumed to be relatively constant throughout the year (T_{deep} in Leach and Moore, 2015), was determined by regressing mean daily air temperatures monitored at East Creek against mean daily air temperature at the MKRF headquarters. The relationship was then applied to the full record of mean daily air temperatures at the MKRF headquarters. From this record, the long-term mean air temperature was calculated. In addition, a standard geothermal temperature gradient of 25 °C per 1000m depth into the earth surface (Wood & Hewett, 1982) was applied to the long-term mean, since T_{deep} was set at 15 m below the ground surface.

For the remaining parameters of the hillslope throughflow temperature model, the 30 behavioural parameter sets determined from the generalized likelihood uncertainty estimate calibration (GLUE; Beven and Binley, 1992) of the hillslope throughflow temperature model in Leach and Moore (2015), which was conducted at Griffith Creek during winter 2011–2012, were used herein to simulate stream temperature at East Creek. Of the 30 behavioural parameter sets, nine resulted in unrealistic prolonged periods of zero discharge when used to simulate stream flow at East Creek. This unrealistic behaviour is likely due to the hillslope throughflow model being calibrated only for winter conditions, as well as potential differences in hydrology parameterization between East and Griffith creeks. These nine parameter sets resulted in unreasonable stream temperature predictions and were removed from subsequent analyses.

Finally, two remaining parameters specific to the stream temperature channel processes (k_{bed} and d_0) were calibrated using 2011 and 2012 stream temperature observations from East Creek. Model predictions of hourly stream temperature among the 21 hillslope throughflow temperature parameter sets were always within 0.75 °C for given d_0 and k_{bed} values; therefore, the number of simulations in the calibration was constrained by only considering one of the 21 parameter sets. One thousand parameter values randomly sampled from a range of d_0 between 0 to 0.15 m and a range of k_{bed} between 0.1 and 40 W m⁻² °C⁻¹ were considered in the calibration. The stream temperature model was initiated by simulating for the year 1963 ten times in order to remove any influence of initial conditions and then was used to simulate 1964 to 2012. The predictions for 2011 and 2012 were compared to observed stream temperatures from East Creek. Five goodness of fit statistics

TABLE 1 List of parameters used in the coupled hydrologic and stream temperature model

Parameter	Symbol	Units	Value	Source
<i>Canopy interception routine</i>				
Snow/rain threshold temperatures	TT_1, TT_2	°C	0, 0	Wigmsta, Vail, and Lettenmaier (1994)
Mean evaporation rate from saturated canopy	\bar{E}	mm hr ⁻¹	0.335	Donnelly-Makovecki and Moore (1999)
Liquid storage capacity	C_l	mm	2.31	Donnelly-Makovecki and Moore (1999)
Canopy gap fraction	f_g		0.203	Donnelly-Makovecki and Moore (1999)
Snow canopy interception efficiency	e_{int}		see Equation (A10)	Martin et al. (2013)
Canopy snow storage capacity	C_s	mm	50	Martin et al. (2013)
Canopy melt factor	α	mm °C ⁻¹ hr ⁻¹	0.08	Moore (1993)
Forest canopy emissivity	ϵ_f		0.95	Oke (1987)
Snow surface emissivity	ϵ_s		0.98	Oke (1987)
<i>Throughflow discharge and temperature routine</i>				
Primarily taken from Leach and Moore 2015). See for list of parameters, values, and details.				
Mean hillslope angle		°	10.6	5-m catchment digital elevation model
<i>Streamflow generation</i>				
Discharge–channel volume relationship	a		0.6	Leach and Moore (2014)
Discharge–channel volume relationship	b		0.22	Leach and Moore (2014)
Mean residual stream depth	\bar{d}_0	m	0–0.15	calibrated
<i>Channel heat budget</i>				
Stream albedo	α		0.05	Oke (1987)
Forest canopy emissivity	ϵ_f		0.95	Oke (1987)
Stream surface emissivity	ϵ_w		0.97	Oke (1987)
Effective stream bed transfer	k_{bed}	W m ⁻² °C ⁻¹	0.1–40	calibrated
Cross-sectional area of bed	A_{bed}	m ²	stream width × 0.5	Guenther et al. (2014)
Bed porosity	ϕ_{bed}		0.3	Freeze and Cherry (1979)
Bed mineral density	ρ_m	kg m ⁻³	2650	Campbell and Norman (1998)
Specific heat of mineral particles	c_{pm}	J kg ⁻¹ °C ⁻¹	870	Campbell and Norman (1998)

were calculated to compare hourly predicted and observed stream temperatures: (a) Nash-Sutcliffe efficiency (NSE; Nash and Sutcliffe, 1970), (b) coefficient of determination (R^2), (c) root mean square error (RMSE), (d) mean absolute error (MAE), and (e) mean bias error (MBE). A \bar{d}_0 of 0.08 m and a k_{bed} of 25 W m⁻² °C⁻¹ maximized NSE and R^2 and minimized RMSE, MAE, MBE and were therefore used in all subsequent analyses.

Both discharge and stream temperature predictions made by the model were evaluated against observations made at East Creek. Similar to the calibration procedure, the stream temperature model was initiated by simulating 1963 ten times and then used to simulate the period of 1964 to 2013. Mean daily discharge (L s⁻¹) simulated by the model was evaluated against observed discharge for 2011 and 2012. Mean daily stream temperature simulated by the model was evaluated against observed stream temperature for 1998 to 2001. For each year of evaluation, NSE, R^2 , RMSE, MAE, and MBE were calculated.

4.3 | Groundwater aquifer

As will be shown, the model consistently overpredicted stream temperature during low-flow periods in late summer. It was hypothesized that the overprediction is a result of the model not accounting for subsurface inflow contributions from deep groundwater sources characterized by stable thermal regimes. Discrete groundwater seeps and springs are known to be a significant input during very low flows at

other catchments within MKRF (Guenther et al. 2014). To explore the validity of this hypothesis, we added a representation of a deeper groundwater flow path to the model. Because no information is available to support the specification of the structure of a groundwater reservoir, we made some ad hoc assumptions that are plausible given the soils and geology of the catchment.

The hypothesized groundwater flow path was represented, for simplicity, using a linear reservoir. The rate of change in water storage of the aquifer reservoir (dS_{gw}/dt in m s⁻¹) is

$$\frac{dS_{gw}}{dt} = q_{d,1} \cdot f_{gw} - q_{gw}, \quad (9)$$

where S_{gw} is the water storage depth (m) of the aquifer, $q_{d,1}$ is the rate of water flow from the duff layer to the mineral soil layer for the upper hillslope reservoir (Leach & Moore, 2015) in m s⁻¹, f_{gw} is the fractional area of the upper hillslope reservoir for which infiltrating water is diverted to the aquifer reservoir, and q_{gw} is the rate of water input entering the stream from the aquifer (m s⁻¹). The rate of water input entering the stream from the aquifer was calculated as

$$q_{gw} = k \cdot S_{gw}, \quad (10)$$

where k is the reservoir outflow coefficient (s⁻¹). For this exercise, k was set equal to the equivalent of a time constant of 1 year.

The advective flux associated with the groundwater input to the stream (Q_{gw} , in W m⁻²) was calculated as

$$Q_{gw} = \rho_w c_w q_{gw} T_{gw}, \quad (11)$$

where ρ_w is the density of water (kg m^{-3}), c_w is the specific heat capacity of water ($\text{J kg}^{-1} \text{C}^{-1}$), and T_{gw} is the groundwater temperature ($^{\circ}\text{C}$).

Three scenarios for the amount of upper hillslope water inputs diverted to the groundwater aquifer (f_{gw}) were considered: 0.1, 0.2, and 0.3. Two scenarios for T_{gw} were considered: (a) T_{gw} was assumed to be equal to the long term mean annual air temperature and did not vary in time, and (2) T_{gw} was estimated using a harmonic function to approximate seasonal temperature variations. The harmonic function used was Stallman's equation (Stallman, 1965) calibrated to groundwater seep temperature data from MKRF (Guenther et al. 2014). See Kurylyk et al. (2015) for details on Stallman's equation as applied to stream temperature modelling. The resulting modelled stream temperature for these scenarios were evaluated against observed stream temperature at East Creek.

5 | RESULTS

5.1 | Hourly air temperature, incoming solar radiation, and snow

Compared to observations, predicted hourly air temperature below the forest canopy at East Creek had RMSE of $1.6\text{ }^{\circ}\text{C}$, MBE of $0.2\text{ }^{\circ}\text{C}$, MAE of $1.1\text{ }^{\circ}\text{C}$, R^2 of 0.81, and NSE of 0.81. Predicted hourly air temperatures tended to exhibit more dynamic diurnal patterns than observed air temperatures (Figure 4). Predicted hourly incoming solar radiation reaching the stream surface had RMSE of 4.1 W m^{-2} , MBE of 1.0 W m^{-2} , MAE of 2.5 W m^{-2} , R^2 of 0.59, and NSE of 0.51 when compared to observations (Figure 5). Differences of up to 50 W m^{-2} were calculated between observed and predicted incoming solar radiation for specific hours of the day and during periods associated with clear sky conditions.

Predicted hourly SWE on the ground from the canopy interception model was compared against observed periods of snow cover derived from time-lapse images from the East Creek outlet (295 m) and from the Griffith Creek forest meteorological site (440 m), which bracket the elevation range of the East Creek catchment (Figure 6). The differences

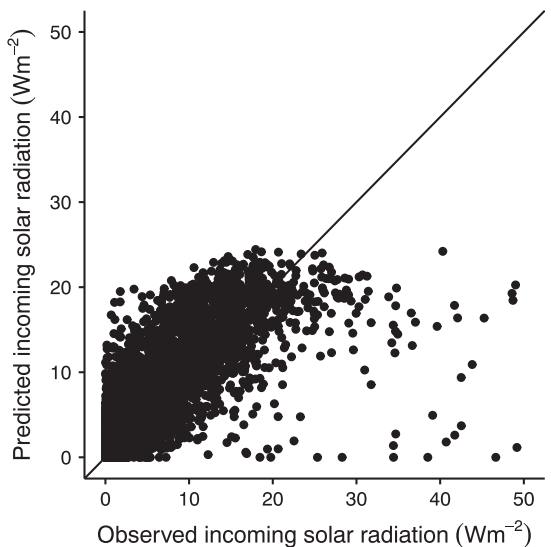


FIGURE 5 Hourly predicted versus observed incoming solar radiation at the Griffith Creek forested site for July 2011 to May 2013. Black line is the 1:1 line

in observed snow cover between the East Creek outlet and Griffith Creek forest site highlight the influence of elevation on snow cover in this region. Generally, the model successfully predicted snow during observed snow cover periods; however, the model also predicted snow accumulation for a number of events when no snow was observed at the monitoring location. These events were primarily characterized by predicted maximum SWE of 2 mm or less and persisted for a couple days, although the predicted snow accumulation event in late January 2013 did reach a maximum SWE of 8 mm and snow cover persisted for 1 to 2 weeks despite no observed snow accumulation during that time.

5.2 | Discharge

Modelled mean daily discharge for East Creek was consistently lower than observed mean daily observed discharge (Figure 7), as indicated by MBE of -14 and -20 L s^{-1} for 2011 and 2012, respectively (Table 2).

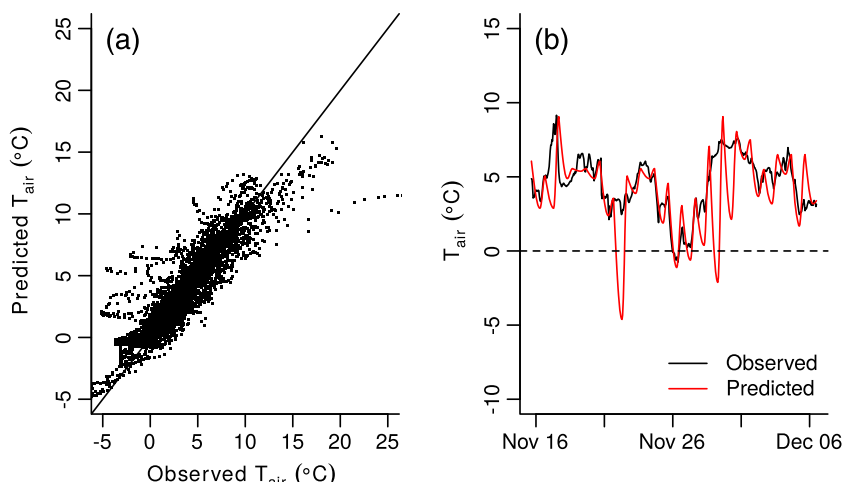


FIGURE 4 Predicted versus observed hourly air temperature for the East Creek forest site for October 2012 to May 2013. Panel (a) shows a scatterplot of hourly air temperatures. Black line is the 1:1 line. Panel (b) shows an example time series for November 16 to December 6, 2012

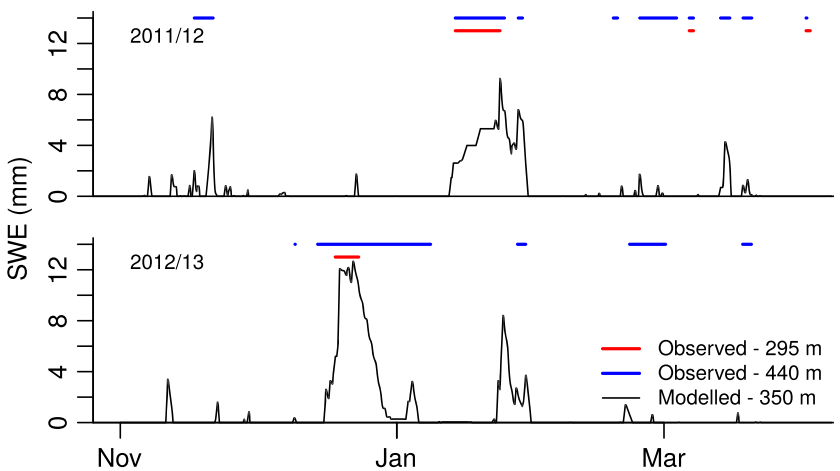


FIGURE 6 Modelled hourly snow water equivalent (mean catchment elevation 350; black line) and three-hr interval observed snow cover at the East Creek outlet (elevation 295 m; red line) and at the Griffith Creek forest meteorological station (elevation 440 m; blue line) for the 2011–2012 and 2012–2013 periods

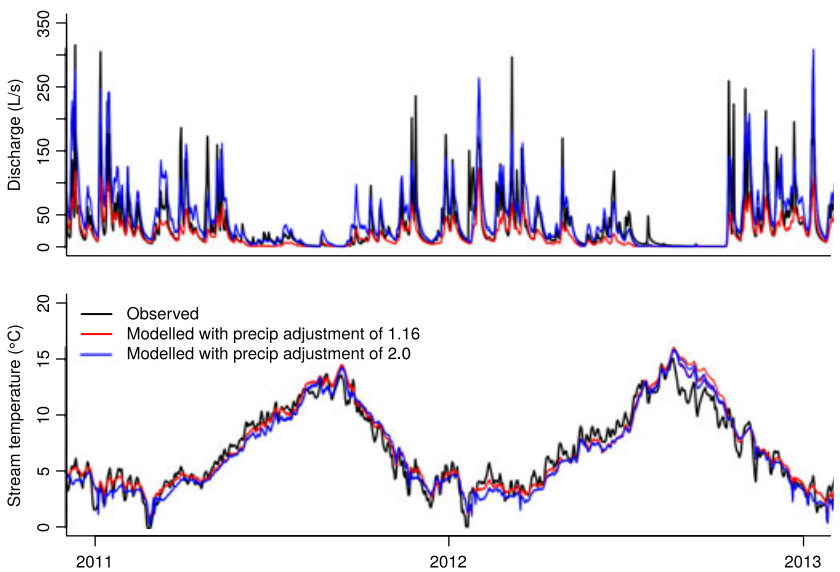


FIGURE 7 Observed versus modelled mean daily discharge for East Creek during 2011 and 2012. Observed discharge is shown in black. Modelled discharge using a precipitation adjustment of 1.16 to account for elevation differences between the MKRF headquarters meteorological station is shown in red. Modelled discharge using a precipitation adjustment of 2.0 to account for elevation differences between the MKRF headquarters meteorological station is shown in blue

The model generally underpredicted event peak flows at East Creek but captured the timing of events, recession limbs, and low-flow conditions. Considering both 2011 and 2012, RMSE, R^2 , and NSE ranged between $32\text{--}39 L s^{-1}$, 0.59–0.65, and 0.27–0.34, respectively. When using a precipitation multiplier of 2.0, instead of 1.16, observed discharge was in better agreement (RMSE = $28\text{--}29 L s^{-1}$; MBE = 6–12 $L s^{-1}$; R^2 = 0.64–0.68; NSE = 0.50–0.62).

5.3 | Stream temperature

The optimum calibration of parameters d_0 and k_{bed} in the stream temperature model resulted in reasonable predictions of daily mean stream temperature when considering the goodness of fit statistics (Table 2), although the model tended to overpredict daily mean stream temperature by up to $3 ^{\circ}C$ during late summer low streamflow conditions

(Figure 7). Daily mean stream temperature predictions made using a precipitation factor of 2.0 compared to 1.16 were similar, although stream temperatures were on average about $0.3 ^{\circ}C$ lower throughout the year when using the 2.0 multiplier. Daily mean stream temperature predictions during the evaluation period (1998 to 2001) using a precipitation multiplier of 1.16 had similar goodness of fit results as the calibration period (Table 2). Modelled stream temperature generally captured the temporal variability in observed stream temperature (Figure 8). Similar to the calibration period, the model tended to consistently overpredict stream temperatures during low-flow periods typically during late summer (Figure 9). This overprediction was most pronounced in 1998 and 2000.

Advection associated with throughflow inputs was the dominant simulated energy input to the stream except during low streamflow periods when the surface energy fluxes dominated the stream energy

TABLE 2 Summary of goodness of fit statistics, root mean square error (RMSE), mean bias error (MBE), mean absolute error (MAE), coefficient of determination (R^2), and Nash-Sutcliffe efficiency (NSE), for East Creek discharge and stream temperature predictions during the calibration and evaluation periods

Year	RMSE	MBE	MAE	R^2	NSE
<i>Stream temperature (°C) calibration using $P \times 1.16$</i>					
2011	0.74–0.76	0.18–0.22	0.60–0.63	0.96	0.95–0.96
2012	1.02–1.21	0.10–0.23	0.82–0.92	0.92–0.94	0.88–0.91
<i>Stream temperature (°C) during calibration period using $P \times 2.0$</i>					
2011	0.89–0.92	(-0.15)–(-0.12)	0.77–0.80	0.93–0.94	0.93–0.94
2012	1.08–1.21	(-0.17)–(-0.09)	0.90–0.99	0.92–0.93	0.88–0.90
<i>Stream temperature (°C) evaluation using $P \times 1.16$</i>					
1998	1.09–1.24	0.31–0.40	0.83–0.92	0.92–0.93	0.89–0.91
1999	0.88–0.91	0.15–0.20	0.64–0.66	0.92–0.93	0.92
2000	0.84–0.86	0.07–0.10	0.68–0.70	0.93–0.94	0.93
2001	0.57–0.60	0.16–0.19	0.47–0.48	0.97	0.96–0.97
<i>Discharge (L/s) evaluation using $P \times 1.16$</i>					
2011	32	-14	16	0.59–0.60	0.33–0.34
2012	39	-20	21	0.64–0.65	0.27–0.29
<i>Discharge (L/s) evaluation using $P \times 2.0$</i>					
2011	28	12	18	0.64–0.66	0.50–0.51
2012	29	6	18	0.66–0.68	0.61–0.62

Note. The range reports the minimum and maximum value for the 21 parameter sets used to run the model. Entries with a single value indicate that all 21 parameter sets resulted in that value given the significant figures reported here. Stream temperature and discharge for 2010 and 2011 were evaluated for their sensitivity to the precipitation correction factor used to account for elevation differences between the Environment Canada climate station and East Creek using either $P \times 1.16$ or $P \times 2.0$. Note that discharge was calibrated to Griffith Creek discharge for the period of October 2011 to April 2012, and no calibration of discharge was done directly for East Creek.

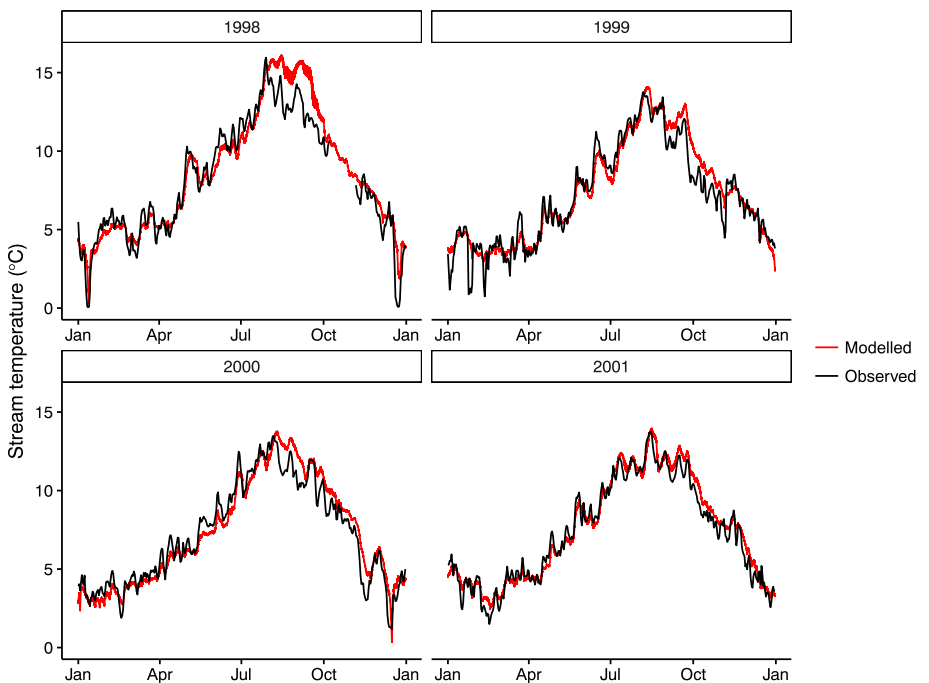


FIGURE 8 Observed (black) versus modelled (red) mean daily stream temperature at East Creek for the model evaluation period (1998 to 2001). The red band represents simulated stream temperature from the 21 behavioural parameter sets

budget (Figure 10). Energy exchanges associated with channel interception precipitation had a minor influence on stream temperature overall; however, during low streamflow conditions and periods of

falling snow, the energy exchange associated with channel interception of snow functioned as a heat sink and resulted in sharp decreases in hourly stream temperature (Figure 11).

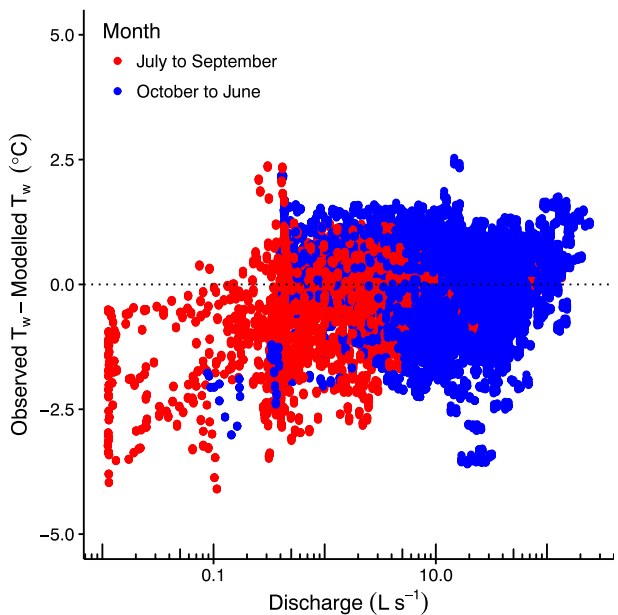


FIGURE 9 Mean daily stream temperature model residuals (observed T_w minus modelled T_w) versus modelled stream discharge for 1998 to 2001 and 2011 and 2012

5.4 | Groundwater aquifer

Three groundwater fractions and two groundwater temperature scenarios were considered for the groundwater model addition. The values for f_{gw} tested (0.1, 0.2, and 0.3) correspond to groundwater contributions to annual streamflow of 6% ($\pm 4\%$), 12% ($\pm 7\%$), and 18% ($\pm 11\%$), respectively. The variability reflects different upper hillslope areas from the original throughflow temperature model calibration (Leach & Moore, 2015). Adding the groundwater component improved stream temperature predictions (Table 3), particularly during the summer months (Figure 12). Specifying a seasonally variable groundwater temperature provided slightly better predictions than a constant groundwater temperature. Stream temperature predictions were

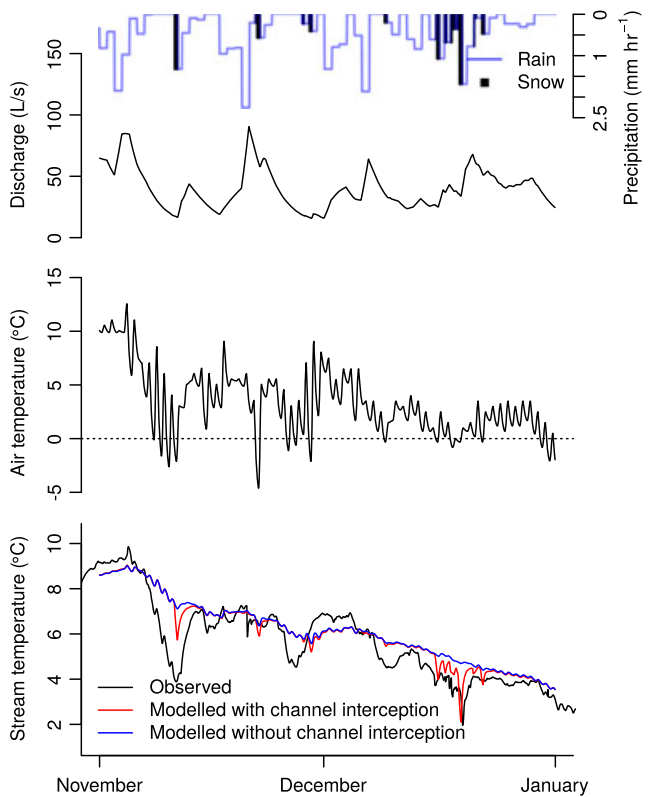


FIGURE 11 Top panel shows modelled hourly discharge, rainfall (blue), and snowfall (black) at East Creek for November 2011 to January 2012. Middle panel shows modelled hourly air temperature for reference. Bottom panel shows hourly observed stream temperature (black), modelled stream temperature accounting for channel interception (red), and modelled stream temperature without channel interception (blue) at East Creek for November 2011 to January 2012

mostly improved for f_{gw} values around 0.1 to 0.2, and model performance dropped with relatively large groundwater contributions ($f_{gw} = 0.3$).

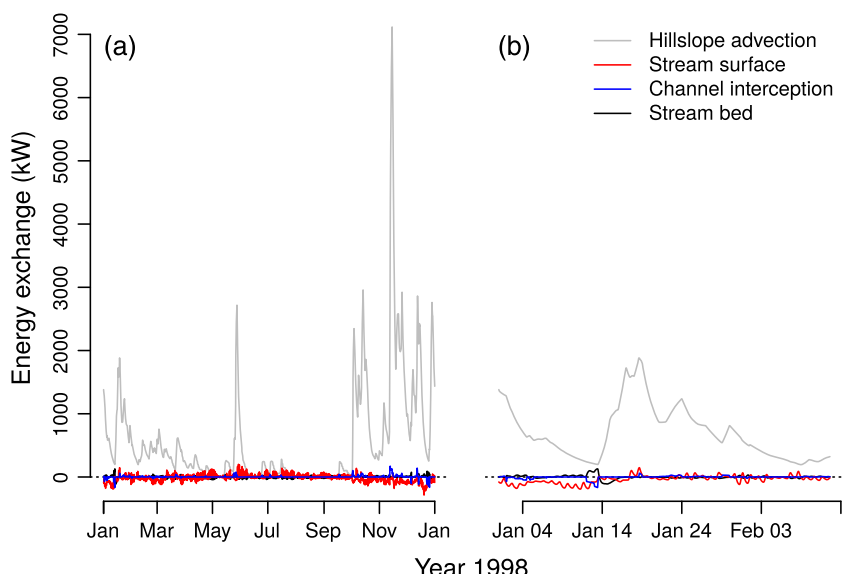


FIGURE 10 Simulated hourly energy exchanges (kW) for the stream temperature model for (a) entire 1998 and (b) a 5-week subset of 1998. Energy exchanges are advection associated with throughflow inputs from the hillslope (grey), stream surface energy exchanges include short- and long-wave radiation (red), channel precipitation interception (blue), and energy exchange with the stream bed (black)

TABLE 3 Summary of goodness of fit statistics, root mean square error (RMSE), mean bias error (MBE), mean absolute error (MAE), coefficient of determination (R^2), and Nash-Sutcliffe efficiency (NSE), for East Creek stream temperature predictions for 1998 to 2001 using (a) a baseline model without a groundwater aquifer component (top row), (b) two groundwater temperature (T_{gw}) scenarios (constant in time and seasonally varying), and (c) three groundwater contribution scenarios where a fraction of the water infiltrating the upper hillslope reservoir is diverted to the groundwater aquifer (f_{gw})

T_{gw}	f_{gw}	RMSE	MBE	MAE	R^2	NSE
None	0	0.89	0.21	0.67	0.94	0.93
Constant	0.1	0.79	0.05	0.61	0.94	0.94
Constant	0.2	0.93	-0.03	0.70	0.94	0.92
Constant	0.3	1.09	-0.06	0.82	0.93	0.89
Seasonal	0.1	0.78	0.06	0.60	0.95	0.94
Seasonal	0.2	0.87	-0.004	0.66	0.94	0.93
Seasonal	0.3	0.98	-0.04	0.74	0.94	0.91

6 | DISCUSSION

6.1 | Snow and discharge predictions

Prediction of SWE and associated periods of snow cover generally agreed with snow cover observations made using time-lapse images. However, the model predicted a number of shallow snow packs (< 2 mm SWE) when no snow cover was observed (Figure 6). These shallow snow pack prediction errors may be a result of errors in downscaling daily precipitation and air temperature to hourly values. For example, down-scaled hourly air temperature tended to be underestimated during nighttime (Figure 4). During periods when mean daily air temperatures

are around 0 °C, these underpredictions may result in rain being simulated as snow. In addition, total daily precipitation was assumed to be equally distributed throughout the hours of the day; therefore, errors in SWE predictions could be compounded if precipitation was erroneously assumed to fall during hours of the day when air temperatures were below 0 °C. These uncertainties in snow predictions are mostly associated with short-lived shallow snow packs, which appear to have a minor influence on subsurface water temperatures (Leach & Moore, 2015).

The model consistently underestimated discharge at East Creek, with NSE ranging between 0.27 and 0.34. There are a number of error sources that could explain the differences in modelled and observed discharge. Potential sources of error include uncertainty in (a) transposing Griffith Creek hydrologic parameterization to East Creek, (b) precipitation inputs, and (c) discharge rating curves. The hydrologic runoff component of the model was calibrated for Griffith Creek (Leach & Moore, 2015) and may not be entirely suitable for application at East Creek. Donnelly-Makovecki and Moore (1999) used a similar three reservoir model to predict discharge at East Creek and another headwater catchment at MKRF using a hierarchical testing framework (Klemeš, 1986). Their model performances were greater than those in this study, with NSE in the range of 0.59 to 0.87. Modelled discharge in our study exhibited similar runoff timing as observed discharge and the modelled errors were primarily due to underestimating discharge magnitude during storm events. This consistent underprediction suggests the errors are primarily associated with uncertainty in model parameters or inputs that influence the catchment water balance. Elevation differences in precipitation were accounted for by

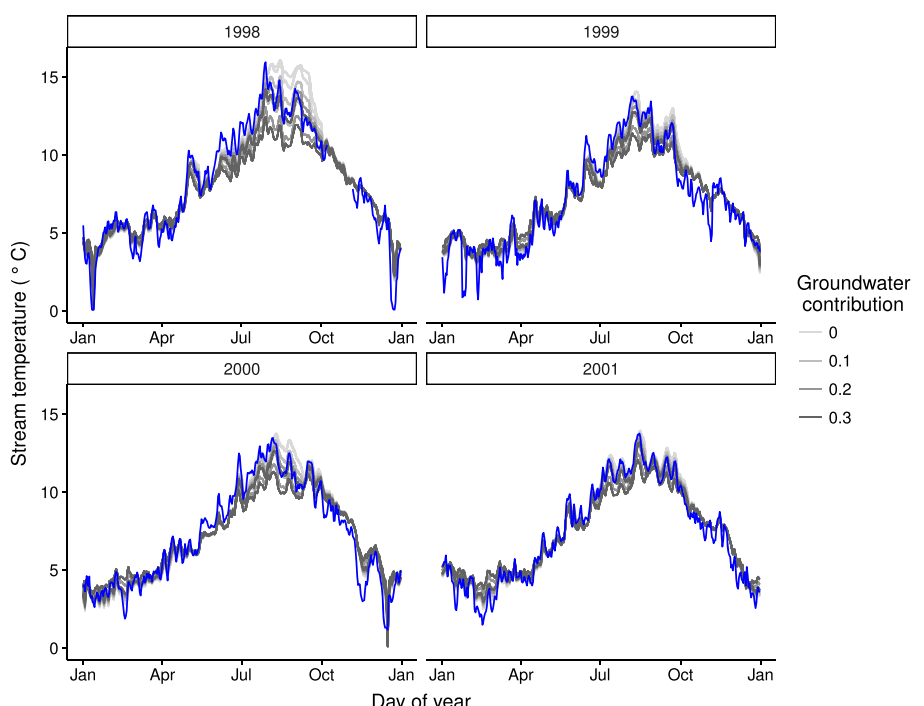


FIGURE 12 Observed (blue) versus modelled (grey) mean daily stream temperature at East Creek for the model evaluation period (1998 to 2001). The grey scale represents the fraction of upslope water that is diverted to the groundwater reservoir (f_{gw}) from 0 (light grey) to 0.3 (dark grey). Variations in predicted stream temperature for each groundwater contribution group reflect differences in the throughflow temperature model calibration. The simulations shown here are based on seasonally varying groundwater temperature

applying a correction factor based on precipitation and throughfall data collected by Donnelly-Makovecki and Moore (1999). It is possible that this correction factor underestimates total precipitation inputs at East Creek. When using a precipitation correction factor of 2.0, agreement between observed and modelled discharge was improved. A likely source of error for the streamflow predictions is the parameterization of the discharge rating curves for East Creek (Beven, Buytaert & Smith, 2012). Historic rating curves have been established for a number of streams in MKRF; however, replicated manual discharge measurements made at Griffith Creek used to build an independent rating curve (Leach & Moore, 2014) suggested that the historic rating curve for Griffith Creek was in error at times by up to 50%. Therefore, uncertainties in the rating curve for East Creek may be a cause for differences between modelled and observed discharge.

6.2 | Stream temperature predictions and process insight

Modelled stream temperature agreed closely with measurements made at the East Creek outlet during the 1998–2001 evaluation period. The model generally predicted the pattern and magnitude of stream temperature, despite the errors in modelled discharge outlined above. Errors in discharge predictions should have consequences for stream temperature predictions, since errors in the volume of water in the channel could result in incorrectly simulated stream temperatures even if the remaining energy fluxes are accurately determined. As long as the throughflow temperatures are relatively accurate, this source of error will be more pronounced during periods of low flow than during high-flow periods. Modelled discharge errors are primarily due to underestimation of event peakflow magnitude; therefore, it appears that stream temperature predictions are relatively insensitive to these errors, as long as the timing of runoff is accurate, since the stream energy budget will be dominated by advection associated with throughflow regardless of whether the magnitude of that flux is underestimated (Leach & Moore, 2014). Overall, the model predicted stream temperature accurately and the relative importance of the energy exchanges simulated by the model was consistent with field-based results from diagnostic energy budget analyses for Griffith Creek for both summer and winter (Guenther, 2007; Leach & Moore, 2014). The ability of the model to reproduce both event-scale and seasonal variability in stream temperature suggests that the dominant processes controlling stream temperature, namely, advection associated with throughflow inputs during high flows and surface energy fluxes during low-flow periods, can be generalized for headwater catchments in this region of the Pacific Northwest.

There was consistent overprediction of stream temperature during late summer periods. This overprediction was most pronounced during the 1998 and 2000 evaluation period and is associated with periods of extended low streamflow conditions. This overprediction could be explained by the assumption that all lateral subsurface inputs to the channel occur via shallow throughflow, which has a relatively dynamic thermal regime. After identifying the modelling overprediction failure, a simple groundwater reservoir was added to the model to incorporate contributions from deeper sources, which have a stable thermal regime

and are known to be a significant input during very low flows at other catchments within MKRF (Guenther et al. 2014). Adding the groundwater reservoir improved the model predictions, particularly during the summer, which is consistent with the assumption that groundwater discharge should have a relatively large influence on stream temperature measured at the catchment outlet during low streamflow conditions compared to periods with higher streamflow. The simple representation of groundwater in the model assumes that the aquifer is recharged by precipitation falling on the catchment. It is possible that groundwater discharge from deeper flow paths originates from outside the catchment (Welch, Allen &, van Meerveld, 2012). In addition, the model overprediction could have also resulted from other model structure errors. For example, it is possible that the representation of heat exchange between the bed and stream may have underestimated this term, particularly in parts of the reach with groundwater discharge zones or substantial hyporheic exchange (Story et al., 2003; Briggs, Lautz, Buckley, & Lane, 2014; Caissie, Kurylyk, St-Hilaire, El-Jabi, & MacQuarrie, 2014; Kurylyk, Moore, & MacQuarrie, 2016).

Heat advected by channel-intercepted precipitation is generally considered to be a minor heat budget term and is often neglected in most heat budget studies (Webb & Zhang, 1999). During the model development phase, an earlier version of the model did not include channel interception and failed to capture the rapid decreases in stream temperature observed during periods of low streamflow conditions and snowfall. By including channel-intercepted precipitation and its associated heat flux in the model, we were able to replicate these stream temperature patterns, although the duration and magnitude were not always simulated. Part of this disagreement could reflect the challenges of modelling snow dynamics in the transient snow zone using spatially extrapolated and temporally downscaled air temperature data. This result suggests that channel interception of snowfall may be important, particularly during low-flow periods, when the energy consumed for the phase change from solid to liquid reduces stream temperatures.

6.3 | Comparison to other stream temperature models

A variety of process-based stream temperature models exist that couple hydrologic and thermal processes (Morin & Couillard, 1990; Bicknell, Imhoff, Kittle, Jobes, & Donigian, 2001; Boyd & Casper, 2003; Allen, Dietrich, Baker, Ligon, & Orr, 2007; Haag & Luce, 2008; Ficklin, Luo, Stewart, & Maurer, 2012; Loinaz, Davidsen, Butts, & Bauer-Gottwein, 2013; Null, Viers, Deas, Tanaka, & Mount, 2013; MacDonald et al., 2014a; Sun et al., 2015). We previously showed that these models either cannot account for the role of transient snow cover on throughflow temperatures or inaccurately estimate throughflow temperature by up to 5 °C. As illustrated here and in a previous field-based study (Leach & Moore, 2014), accurate simulation of lateral throughflow temperature is critical for predicting full year stream temperature in forested headwater streams in coastal regions of the Pacific Northwest. Working in a catchment with a seasonally continuous snowpack, Gallice et al. (2016) demonstrated that the effect of lateral throughflow was strong during the spring melt period, suppressing the seasonal increase in stream temperature.

Many process-based stream temperature models require a user-supplied or measured stream temperature for the upstream boundary in order to initiate the model (e.g., Boyd & Casper, 2003; MacDonald et al., 2014a). Other models, such as DHSVM-RBM (Sun et al. 2015), use empirical relationships between air and water temperatures (e.g., Mohseni, Stefan, & Erickson, 1998) to estimate upstream water temperatures. Both these approaches limit the usefulness of these models for simulating stream temperature response to land-use and climatic changes for scenarios where the initiation stream temperatures would also be expected to respond. The model developed in this study is reasonably computationally efficient yet is strongly process-based and thus enhances our ability to predict the effects of climate and land-use change on stream temperature in the upper portions of the stream network.

Recent developments in coupled hydrology and stream temperature models include StreamFlow (Comola et al. 2015; Gallice et al. 2016), a model designed for application in mesoscale snow-dominated alpine catchments. The current version of StreamFlow provides three approaches to simulate throughflow temperature: (a) a simplified energy balance approach with some similarities to the throughflow routine outlined in our study, (b) the approach used by the Hydrological Simulation Program–Fortran (HSPF; Bicknell et al., 2001), and (c) an approach based on simulated soil temperatures. Gallice et al. (2016) found that downstream daily mean stream temperature predictions varied by up to 4 °C depending on the throughflow temperature approach used. Our results and those from Gallice et al. (2016) highlight the importance of throughflow advection on stream thermal regimes in mountainous environments and a need to properly represent this term in stream temperature models.

There are a number of limitations of the stream temperature model presented here. The model is spatially lumped and, therefore, cannot be used in catchments with considerable spatial heterogeneity in terms of dominant runoff processes or elevation and its influence on snow accumulation. In addition, the model would not provide suitable predictions for streams dominated by deep regional groundwater inputs, extensive hyporheic exchange, or extended seasonal ice formation. Due to the importance of the advection associated with throughflow dominating the thermal regimes of these headwater catchments, it is important to adequately calibrate the throughflow temperature model component (Leach & Moore, 2015). Despite these limitations, the model appears reasonably robust to the estimation of hourly input from daily values and useful for simulating stream temperature for small forested headwater catchments in the rain-on-snow zone of the Pacific Northwest. These headwater catchments are estimated to drain up to 80% of catchment area in the Pacific Northwest (Gomi, Sidle, & Richardson, 2002) and provide important habitat for aquatic organisms that are thermally sensitive (Olson, Anderson, Frissell, Welsh, & Bradford, 2007). In addition, the stream temperature of headwater streams sets the upstream boundary conditions for thermal regimes of downstream reaches.

7 | CONCLUSIONS

A catchment-scale stream temperature model was developed to simulate streamflow generation and stream temperature for forested

headwater catchments in the rain-on-snow zone. Despite limited catchment-specific calibration, the model generally predicted stream temperature accurately over the full annual cycle (annual RMSE between 0.57 and 1.24 °C, and NSE between 0.89 and 0.97). The model's robustness likely reflects the fact that process representations were as strongly based on physical principles as was possible given the limited driving data available. The model highlighted the dominance of lateral advection as a control on stream temperature in montane headwater streams, particularly during the winter wet season.

There were two notable situations in which the model did not perform well. The model overpredicted mean daily summer stream temperatures by up to 3 °C for late summer periods characterized by extended low streamflow conditions. This failure is believed to reflect a shift from shallow throughflow to deeper subsurface flow paths as a streamflow source. Adding a simple groundwater reservoir in order to explore this hypothesis resulted in improved stream temperature predictions, particularly during the summer periods. Future work should focus on developing better representations of subsurface flow contributions and their thermal influence in headwater catchments. The other failure was an inability to simulate depressed stream temperature during snowfall events. Incorporating snowfall into the channel improved the simulations, supporting the potentially important, but previously unrecognized, role of this process. This study illustrates the utility of physically based models as a tool for learning about processes, especially by focusing on model failures.

ACKNOWLEDGMENTS

This study is part of a broader project funded by a Natural Sciences and Engineering Research Council (NSERC) Discovery grant to R.D.M. J.A.L. was supported by a Canadian Graduate Scholarship (NSERC), Donald Gray Scholarship in Canadian Hydrology (Canadian Geophysical Union), and Dillon Consulting Scholarship (Canadian Water Resources Association). Field assistance was provided by Eli Heyman, Spencer Pasieka, Saskia Hövelmann, Derek van der Kamp, Joel Trubilowicz, Justin Knudson, and Kaitlin Kazmierowski. Eric Leinberger created Figure 1. The staff at the Malcolm Knapp Research Forest is greatly appreciated for logistic help. Comments from two anonymous reviewers greatly improved the manuscript.

ORCID

Jason A. Leach  <http://orcid.org/0000-0001-6639-7993>

REFERENCES

- Allen, D., Dietrich, W. E., Baker, P. F., Ligon, F., & Orr, B. (2007). Development of a mechanistically based, basin-scale stream temperature model: Applications to cumulative effects modeling, *Proceedings of the Redwood Region Forest Science Symposium: What Does the Future Hold* (pp. 11–24). Albany, California: Forest Service, US Department of Agriculture.
- Arismendi, I., Johnson, S. L., Dunham, J. B., & Haggerty, R. (2013). Descriptors of natural thermal regimes in streams and their responsiveness to change in the Pacific Northwest of North America. *Freshwater Biology*, 58(5), 880–894.
- Beacham, T. D., & Murray, C. B. (1990). Temperature, egg size, and development of embryos and alevins of five species of Pacific salmon: A comparative analysis. *Transactions of the American Fisheries Society*, 119, 927–945.

- Beschta, R. L., Bilby, R. E., Brown, G., Holtby, L. B., & Hofstra, T. D. (1987). Stream temperature and aquatic habitat: Fisheries and forestry interactions. *Streamside Management: Forestry and Fishery Interactions* (pp. 191–232), number 57. Seattle, Washington: University of Washington, Institute of Forest Resources.
- Beven, K., & Binley, A. (1992). Future of distributed models: Model calibration and uncertainty prediction. *Hydrological Processes*, 6(3), 279–298.
- Beven, K., Buytaert, W., & Smith, L. A. (2012). On virtual observatories and modelled realities (or why discharge must be treated as a virtual variable). *Hydrological Processes*, 26, 1905–1908.
- Bicknell, B. R., Imhoff, J. C., Kittle, J. L., Jobes, T. H., & Donigian, A. S. (2001). *Hydrological Simulation Program-Fortran (HSPF) user's manual for release 12*. Athens, GA: US Environmental Protection Agency, National Exposure Research Laboratory.
- Boss, S. M., & Richardson, J. S. (2002). Effects of food and cover on the growth, survival, and movement of cutthroat trout (*Oncorhynchus clarkii*) in coastal streams. *Canadian Journal of Fisheries and Aquatic Sciences*, 59(6), 1044–1053.
- Boyd, M., & Casper, B. (2003). *Analytical methods of dynamic open channel heat and mass transfer: Methodology for the Heat Source Model Version 7.0*. Portland, Oregon: Oregon Department of Environmental Quality.
- Briggs, M. A., Lautz, L. K., Buckley, S. B., & Lane, J. W. (2014). Practical limitations on the use of diurnal temperature signals to quantify groundwater upwelling. *Journal of Hydrology*, 519, 1739–1751.
- Bristow, K. L., & Campbell, G. S. (1984). On the relationship between incoming solar radiation and daily maximum and minimum temperature. *Agricultural and Forest Meteorology*, 31(2), 159–166.
- Brown, G. W. (1969). Predicting temperatures of small streams. *Water Resources Research*, 5(1), 68–75.
- Brown, R. S., Hubert, W. A., & Daly, S. F. (2011). A primer on winter, ice, and fish: What fisheries biologists should know about winter ice processes and stream-dwelling fish. *Fisheries*, 36(1), 8–26.
- Caissie, D., Kurylyk, B. L., St-Hilaire, A., El-Jabi, N., & MacQuarrie, K. T. B. (2014). Stream temperature dynamics and corresponding heat fluxes in small streams experiencing seasonal ice cover. *Journal of Hydrology*, 519, 1441–1452.
- Campbell, G. S., & Norman, J. M. (1998). *An introduction to environmental biophysics* (2nd ed.). New York: Springer-Verlag.
- Cheng, J. D. (1988). Subsurface stormflows in the highly permeable forested watersheds of southwestern British Columbia. *Journal of Contaminant Hydrology*, 3, 171–191.
- Comola, F., Schaeefli, B., Rinaldo, A., & Lehning, M. (2015). Thermodynamics in the hydrologic response: Travel time formulation and application to Alpine catchments. *Water Resources Research*, 51(3), 1671–1687.
- Danehy, R. J., Colson, C. G., & Duke, S. D. (2010). Winter longitudinal thermal regime in four mountain streams. *Northwest Science*, 84(1), 151–158.
- Donnelly-Makovecki, L. M., & Moore, R. D. (1999). Hierarchical testing of three rainfall-runoff models in small forested catchments. *Journal of Hydrology*, 219(3–4), 136–152.
- Durance, I., & Ormerod, S. J. (2007). Climate change effects on upland stream macroinvertebrates over a 25-year period. *Global Change Biology*, 13(5), 942–957.
- Eaton, J., & Scheller, R. (1996). Effects of climate warming on fish thermal habitat in streams of the United States. *Limnology and Oceanography*, 41(5), 1109–1115.
- Ebersole, J., Wigington, Jr, Baker, J., Cairns, M., Church, M., Hansen, B., ..., & Leibowitz, S. (2006). Juvenile coho salmon growth and survival across stream network seasonal habitats. *Transactions of the American Fisheries Society*, 135(6), 1681–1697.
- Ebersole, J. L., Liss, W. J., & Frissell, C. A. (2001). Relationship between stream temperature, thermal refugia and rainbow trout (*Oncorhynchus mykiss*) abundance in arid-land streams in the northwestern United States. *Ecology of Freshwater Fish*, 10(1), 1–10.
- Feller, M. C., & Kimmins, J. P. (1979). Chemical characteristics of small streams near Haney in southwestern British Columbia. *Water Resources Research*, 15(2), 247–258.
- Ficklin, D. L., Luo, Y., Stewart, I. T., & Maurer, E. P. (2012). Development and application of a hydroclimatological stream temperature model within the Soil and Water Assessment Tool. *Water Resources Research*, 48, W01511.
- Freeze, R. A., & Cherry, J. A. (1979). *Groundwater*. Englewood Cliffs: Prentice-Hall.
- Gallice, A., Bavay, M., Brauchli, T., Comola, F., Lehning, M., & Huwald, H. (2016). StreamFlow 1.0: An extension to the spatially distributed snow model Alpine3D for hydrological modeling and deterministic stream temperature prediction. *Geoscientific Model Development*, 9, 4491–4519.
- Garner, G., Malcolm, I. A., Sadler, J. P., Millar, C. P., & Hannah, D. H. (2015). Inter-annual variability in the effects of riparian woodland on micro-climate, energy exchanges and water temperature of an upland Scottish stream. *Hydrological Processes*, 29, 1080–1095.
- Gomi, T., Sidle, R. C., & Richardson, J. S. (2002). Understanding processes and downstream linkages of headwater systems. *BioScience*, 52(10), 905–916.
- Guenther, S. M. (2007). Impacts of partial-retention harvesting with no buffer on the thermal regime of a headwater stream and its riparian zone. (Master's thesis), University of British Columbia.
- Guenther, S. M., Gomi, T., & Moore, R. D. (2014). Stream and bed temperature variability in a coastal headwater catchment: Influences of surface-subsurface interactions and partial-retention forest harvesting. *Hydrological Processes*, 28, 1238–1249.
- Guenther, S. M., Moore, R. D., & Gomi, T. (2012). Riparian microclimate and evaporation from a coastal headwater stream and their response to partial-retention forest harvesting. *Agriculture and Forest Meteorology*, 164, 1–9.
- Haag, I., & Luce, A. (2008). The integrated water balance and water temperature model LARSIM-WT. *Hydrological Processes*, 22, 1046–1056.
- Hannah, D. M., Malcolm, I. A., Soulsby, C., & Youngson, A. F. (2008). A comparison of forest and moorland stream microclimate, heat exchanges and thermal dynamics. *Hydrological Processes*, 22(7), 919–940.
- Harper, M. P., & Peckarsky, B. L. (2006). Emergence cues of a mayfly in a high-altitude stream ecosystem: Potential response to climate change. *Ecological Applications*, 16, 612–621.
- Haught, D. R. W., & van Meerveld, H. J. (2011). Spatial variation in transient water table responses: Differences between an upper and lower hillslope zone. *Hydrological Processes*, 25, 3866–3877.
- Holtby, L. B. (1988). Effects of logging on stream temperatures in Carnation Creek British Columbia, and associated impacts on the coho salmon (*Oncorhynchus kisutch*). *Canadian Journal of Fisheries and Aquatic Sciences*, 45(3), 502–515.
- Hutchinson, D. G., & Moore, R. D. (2000). Throughflow variability on a forested hillslope underlain by compacted glacial till. *Hydrological Processes*, 14(10), 1751–1766.
- Iqbal, M. (1983). *An introduction to solar radiation*. Toronto: Academic Press.
- Isaak, D. J., Wollrab, S., Horan, D., & Chandler, G. (2012). Climate change effects on stream and river temperatures across the northwest U.S. from 1980–2009 and implications for salmonid fishes. *Climatic Change*, 113, 499–524.
- Isaak, D. J., Young, M. K., Luce, C. H., Hostetler, S. W., Wenger, S. J., Peterson, E. E., ..., & Nagel, D. E. (2016). Slow climate velocities of mountain streams portend their role as refugia for cold-water biodiversity. *Proceedings of the National Academy of Sciences*, 113(16), 4374–4379.
- Johnson, S. L. (2004). Factors influencing stream temperatures in small streams: Substrate effects and a shading experiment. *Canadian Journal of Fisheries and Aquatic Sciences*, 61(6), 913–923.
- Kasten, F., & Young, A. T. (1989). Revised optical air mass tables and approximation formula. *Applied Optics*, 28(22), 4735–4738.
- Kirchner, J. W. (2006). Getting the right answers for the right reasons: Linking measurements, analyses, and models to advance the science of hydrology. *Water Resources Research*, 42(3), W03504.

- Klemeš, V. (1986). Operational testing of hydrological simulation models. *Hydrological Sciences Journal*, 31(1), 13–24.
- Krajina, V. (1965). Biogeoclimatic zones and classification of British Columbia. *Ecology of Western North America*, 1, 1–17.
- Kurylyk, B. L., MacQuarrie, K. T., Caissie, D., & McKenzie, J. M. (2015). Shallow groundwater thermal sensitivity to climate change and land cover disturbances: Derivation of analytical expressions and implications for stream temperature modeling. *Hydrology and Earth System Sciences*, 19(5), 2469–2489.
- Kurylyk, B. L., Moore, R. D., & MacQuarrie, K. T. B. (2016). Scientific briefing: Quantifying streambed head advection associated with groundwater-surface water interactions. *Hydrological Processes*, 30, 978–992.
- Leach, J. A., & Moore, R. D. (2010). Above-stream microclimate and stream surface energy exchanges in a wildfire-disturbed riparian zone. *Hydrological Processes*, 24(17), 2369–2381.
- Leach, J. A., & Moore, R. D. (2011). Stream temperature dynamics in two hydrogeomorphically distinct reaches. *Hydrological Processes*, 25(5), 679–690.
- Leach, J. A., & Moore, R. D. (2014). Winter stream temperature in the rain-on-snow zone of the Pacific northwest: Influences of hillslope runoff and transient snow cover. *Hydrology and Earth System Sciences*, 18, 819–838.
- Leach, J. A., & Moore, R. D. (2015). Observations and modeling of hillslope throughflow temperatures in a coastal forested catchment. *Water Resources Research*, 51, 3770–3795.
- Leach, J. A., Moore, R. D., Hinch, S. G., & Gomi, T. (2012). Estimation of forest harvesting-induced stream temperature changes and bioenergetic consequences for cutthroat trout in a coastal stream in British Columbia, Canada. *Aquatic Sciences*, 74(3), 427–441.
- Lee, R. M., & Rinne, J. N. (1980). Critical thermal maxima of five trout species in the Southwestern United States. *Transactions of the American Fisheries Society*, 109(6), 632–635.
- Lisi, P. J., Schindler, D. E., Cline, T. J., Scheuerell, M. D., & Walsh, P. B. (2015). Watershed geomorphology and snowmelt control stream thermal sensitivity to air temperature. *Geophysical Research Letters*, 42(9), 3380–3388.
- Loinaz, M. C., Davidsen, H. K., Butts, M., & Bauer-Gottwein, P. (2013). Integrated flow and temperature modelling at the catchment scale. *Journal of Hydrology*, 495, 238–251.
- MacDonald, R. J., Boon, S., & Byrne, J. M. (2014a). A process-based stream temperature modelling approach for mountain regions. *Journal of Hydrology*, 511, 920–931.
- MacDonald, R. J., Boon, S., Byrne, J. M., & Silins, U. (2014b). A comparison of surface and subsurface controls on summer temperature in a headwater stream. *Hydrological Processes*, 28, 2338–2347.
- Malard, F., Mangin, A., Uehlinger, U., & Ward, J. (2001). Thermal heterogeneity in the hyporheic zone of a glacial floodplain. *Canadian Journal of Fisheries and Aquatic Sciences*, 58(7), 1319–1335.
- Martin, K. A., Stan, J. T., Dickerson-Lange, S. E., Lutz, J. A., Berman, J. W., Gersonde, R., & Lundquist, J. D. (2013). Development and testing of a snow interceptometer to quantify canopy water storage and interception processes in the rain/snow transition zone of the North Cascades, Washington, USA. *Water Resources Research*, 49(6), 3243–3256.
- Mohseni, O., Stefan, H. G., & Erickson, T. R. (1998). A nonlinear regression model for weekly stream temperatures. *Water Resources Research*, 34, 2685–2692.
- Moore, R. D. (1983). On the use of bulk aerodynamic formulae over melting snow. *Hydrology Research*, 14(4), 193–206.
- Moore, R. D. (1993). Application of a conceptual streamflow model in a glacierized drainage basin. *Journal of Hydrology*, 150(1), 151–168.
- Moore, R. D., Spittlehouse, D. L., & Story, A. (2005a). Riparian microclimate and stream temperature response to forest harvesting: A review. *Journal of the American Water Resources Association*, 41(4), 813–834.
- Moore, R. D., Sutherland, P., Gomi, T., & Dhakal, A. (2005b). Thermal regime of a headwater stream within a clear-cut, coastal British Columbia, Canada. *Hydrological Processes*, 19(13), 2591–2608.
- Morin, G., & Couillard, D. (1990). Encyclopedia of fluid mechanics, surface and groundwater flow phenomena, Chapter 5: Predicting River Temperatures with a Hydrological Model (pp. 171–209). Hudson, Texas: Gulf Publishing Company.
- Nash, J. E., & Sutcliffe, J. V. (1970). River flow forecasting through conceptual models part I-A discussion of principles. *Journal of Hydrology*, 10(3), 282–290.
- Null, S. E., Viers, J. H., Deas, M. L., Tanaka, S. K., & Mount, J. F. (2013). Stream temperature sensitivity to climate warming in California's Sierra Nevada: Impacts to coldwater habitat. *Climatic Change*, 116, 149–170.
- Oke, T. (1987). *Boundary layer climates* (2nd ed.). London, United Kingdom: Halsted Press.
- Olson, D. H., Anderson, P. D., Frissell, C. A., Welsh Jr., H. H., & Bradford, D. F. (2007). Biodiversity management approaches for stream riparian areas: Perspectives for Pacific Northwest headwater forests, microclimate and amphibians. *Forest Ecology and Management*, 246(1), 81–107.
- Penaluna, B. E., Dunham, J. B., Railsback, S. F., Arismendi, I., Johnson, S. L., Bilby, R. E., ... & Skagset, A. E. (2015). Local variability mediates vulnerability of trout populations to land use and climate change. *PloS ONE*, 10(8), e0135334.
- Shuter, B. J., Finstad, A. G., Helland, I. P., Zweimüller, I., & Höller, F. (2012). The role of winter phenology in shaping the ecology of freshwater fish and their sensitivities to climate change. *Aquatic Sciences*, 74, 637–657.
- Soetaert, K., Petzoldt, T., & Setzer, R. W. (2010). Solving differential equations in R: Package deSolve. *Journal of Statistical Software*, 33(9), 1–25.
- Stallman, R. (1965). Steady one-dimensional fluid flow in a semi-infinite porous medium with sinusoidal surface temperature. *Journal of Geophysical Research*, 70(12), 2821–2827.
- Story, A., Moore, R. D., & Macdonald, J. S. (2003). Stream temperatures in two shaded reaches below cutblocks and logging roads: Downstream cooling linked to subsurface hydrology. *Canadian Journal of Forest Research*, 33(8), 1383–1396.
- Sun, N., Yearsley, J., Voisin, N., & Lettenmaier, D. P. (2015). A spatially distributed model for the assessment of land use impacts on stream temperature in small urban watersheds. *Hydrological Processes*, 29, 2331–2345.
- Theurer, F. D., Voos, K. A., & Miller, W. J. (1984). Instream water temperature model. (Technical report): Fort Collins, CO: Fish and Wildlife Service Instream Flow Information Paper 16, FWS/OBS-84/15.
- Thompson, J. C., & Moore, R. D. (1996). Relations between topography and water table depth in a shallow forest soil. *Hydrological Processes*, 10(11), 1513–1525.
- Thornton, P. E., & Running, S. W. (1999). An improved algorithm for estimating incident daily solar radiation from measurements of temperature, humidity, and precipitation. *Agricultural and Forest Meteorology*, 93(4), 211–228.
- Utting, M. G. (1979). The generation of stormflow on a glaciated hillslope in coastal British Columbia. (Master's thesis), University of British Columbia, Vancouver, Canada.
- Wagner, M. J., Bladon, K. D., Silins, U., Williams, C. H. S., Martens, A. M., Boon, S., ... & Anderson, A. (2014). Catchment-scale stream temperature response to land disturbance by wildfire governed by surface-subsurface energy exchange and atmospheric controls. *Journal of Hydrology*, 517, 328–338.
- Webb, B. W., Hannah, D. M., Moore, R. D., Brown, L. E., & Nobilis, F. (2008). Recent advances in stream and river temperature research. *Hydrological Processes*, 22(7), 902–918.
- Webb, B. W., & Zhang, Y. (1999). Water temperatures and heat budgets in Dorset chalk water courses. *Hydrological Processes*, 13(3), 309–321.
- Wehrly, K. E., Wang, L., & Mitro, M. (2007). Field-based estimates of thermal tolerance limits for trout: Incorporating exposure time and temperature fluctuation. *Transactions of the American Fisheries Society*, 136(2), 365–374.

- Welch, L. A., Allen, D. M., & van Meerveld, H. (2012). Topographic controls on deep groundwater contributions to mountain headwater streams and sensitivity to available recharge. *Canadian Water Resources Journal*, 37(4), 349–371.
- Wigmota, M. S., Vail, L. W., & Lettenmaier, D. P. (1994). A distributed hydrology-vegetation model for complex terrain. *Water Resources Research*, 30(6), 1665–1680.
- Wood, J. R., & Hewett, T. A. (1982). Fluid convection and mass transfer in porous sandstones—A theoretical model. *Geochimica et Cosmochimica Acta*, 46(10), 1707–1713.

How to cite this article: Leach JA, Moore D. Insights on stream temperature processes through development of a coupled hydrologic and stream temperature model for forested coastal headwater catchments. *Hydrological Processes*. 2017;31:3160–3177. <https://doi.org/10.1002/hyp.11190>

APPENDIX A: MODEL DESCRIPTION

In the following sections, the equations used to calculate canopy interception and snow accumulation and melt are outlined, followed by the equations used to calculate the water and heat balances of the stream channel.

A.1 | Canopy interception and snow routine

The first step in modelling catchment inputs is to partition precipitation at each hourly time step, $P(t)$, into rainfall, $R(t)$, and snowfall, $SF(t)$ (all in mm), as follows:

$$SF(t) = \begin{cases} P(t) & T_a(t) < TT_1 \\ P(t)(T_a(t) - TT_1)/(TT_2 - TT_1) & TT_1 \leq T_a(t) \leq TT_2 \\ 0 & T_a(t) > TT_2 \end{cases} \quad (A1)$$

and

$$R(t) = P(t) - SF(t), \quad (A2)$$

where $T_a(t)$ is air temperature measured at an open site ($^{\circ}\text{C}$), and TT_1 and TT_2 are threshold temperatures ($^{\circ}\text{C}$). The thresholds were both set to $0\ ^{\circ}\text{C}$, the default values used in the Distributed Hydrology-Soil-Vegetation Model (DHSVM; Wigmota et al., 1994).

Rainfall interception was modelled using approaches based on Donnelly-Makovecki and Moore (1999). For a time step in which the canopy is snow-free throughout, an interim value of canopy liquid water storage is computed as follows:

$$S'_l(t) = S_l(t) + R(t); \quad (A3)$$

where $S'_l(t)$ is the interim liquid storage (mm) at time t , and $S_l(t)$ is the liquid water storage at time t . Evaporation from the canopy, $E(t)$ (mm), during the time step is computed as

$$E(t) = \bar{E}\Delta t \min(1, \bar{S}_l(t)/C_l), \quad (A4)$$

where \bar{E} is the mean evaporation rate from a saturated canopy during rain events (mm/hr), Δt is the length of the time step (hr), $\bar{S}_l(t)$ is the mean of $S_l(t)$ and $S'_l(t)$, and C_l is the liquid storage capacity of the canopy (mm), which is assumed to be constant and independent of presence of

snow in the canopy. The value of \bar{E} was set at 0.335 mm/hr, and C_l was set to 2.31 mm (Donnelly-Makovecki & Moore, 1999).

The interim liquid water storage is updated by subtracting the evaporation:

$$S'_l(t) = S'_l(t) - E(t). \quad (A5)$$

Canopy drip, $TF_d(t)$ (mm), is computed as

$$TF_d(t) = \max(0, S'_l(t) - C_l). \quad (A6)$$

Total throughfall, $TF(t)$ (mm), reaching the ground surface during the time interval is then computed as

$$TF(t) = f_g R(t) + (1 - f_g)TF_d(t), \quad (A7)$$

where f_g is the canopy gap fraction, set to 0.203 (Donnelly-Makovecki & Moore, 1999). The liquid storage at the end of the time interval is computed as

$$S_l(t+1) = S'_l(t) = TF_d(t). \quad (A8)$$

In the snowfall interception routine, an interim value of canopy snow water storage is computed at each time step as follows:

$$S'_s(t) = S_s(t) + e_{int}SF(t), \quad (A9)$$

where $S'_s(t)$ is the interim snow storage (mm), $S_s(t)$ is the snow water storage (mm), and e_{int} is the snow canopy interception efficiency (fraction). Following the results of Martin et al. (2013), the interception efficiency is computed as

$$e_{int} = \begin{cases} 0.8 & S_s(t) < C_s \\ 0 & S_s(t) \geq C_s \end{cases}, \quad (A10)$$

where C_s is the canopy snow storage capacity (mm). Melt of canopy-held snow during the time interval, $M_c(t)$ (mm), is calculated as follows:

$$M_c(t) = \min(S'_s(t), \Delta t \alpha T_a(t)), \quad (A11)$$

where α is a canopy melt factor ($\text{mm} \cdot ^{\circ}\text{C}^{-1} \text{hr}^{-1}$) and $T_a(t)$ is air temperature measured at an open site during the time interval ($^{\circ}\text{C}$). The interim canopy snow storage is updated by subtracting the melt:

$$S'_s(t) = S'_s(t) - M_c(t). \quad (A12)$$

Mass unloading of snow from the canopy is computed as

$$U(t) = \max(0, S'_s(t) - C_s). \quad (A13)$$

The snow storage at the end of the time interval is then

$$S_s(t+1) = S'_s(t) - U(t). \quad (A14)$$

Throughfall of snow (TF_s) reaching the ground surface during the time interval beginning at t is then computed as

$$TF_s(t) = f_g SF(t) + (1 - f_g)(U(t) + SF(t)(1 - e_{int})). \quad (A15)$$

When the canopy holds snow, the routines for handling rain and liquid water storage are the same as in Equations A3 to A7, except that $E(t)$ is set to 0 and Equation A3 is amended as follows:

$$S'_l(t) = S_l(t) + R(t) + M_c(t). \quad (A16)$$

For modelling snowpack water equivalent on the ground, $SWE(t)$ (mm), it is assumed that the snowpack never drops below 0 °C, its liquid water retention capacity is always satisfied, and there is no lag time associated with percolation. Field observations suggest these are reasonable assumptions for the typically shallow snowpacks in the transient snow zone.

At each time step, an interim value of snowpack water equivalent, $SWE'(t)$, is computed as follows:

$$SWE'(t) = SWE(t) + TF_s(t). \quad (\text{A17})$$

Melt rate during the time step, $M(t)$ (mm), is computed as

$$M(t) = \min(SWE'(t), M_p(t)), \quad (\text{A18})$$

where $M_p(t)$ is potential melt (mm), computed as

$$M_p(t) = 1000 \cdot \Delta t \frac{Q_* + Q_h + Q_e + Q_p}{\rho_w L_f}, \quad (\text{A19})$$

where the terms in the numerator represent net radiation (Q_*), the sensible (Q_h) and latent heat (Q_e) fluxes and the sensible heat of precipitation (Q_p), all in W m^{-2} , ρ_w is the density of water (kg m^{-3}), and L_f is the latent heat of fusion (J kg^{-1}). The factor of 1000 is included to convert depth units from m to mm.

Net radiation is computed based on the assumption that solar irradiance below the forest canopy is negligible under the mature forest canopy. This assumption is reasonable based on summer observations from Griffith Creek where below canopy incoming solar radiation was typically less than 40 W m^{-2} at midday (Guenther, 2007). In addition, winter is characterized by low sun angles and frequent cloud cover. Net radiation is computed as

$$Q_* = \varepsilon_f \sigma (T_f(t) + 273.2)^4 - \varepsilon_s \sigma 273.2^4, \quad (\text{A20})$$

where ε_f and ε_s are the emissivities of the forest canopy and snow surface, respectively, σ is the Stefan-Boltzmann constant, and $T_f(t)$ is the air temperature below the forest canopy (°C). The emissivities are set at 0.95 and 0.98 for the forest canopy and snow surface, respectively (Oke, 1987).

The sensible and latent heat fluxes are computed using aerodynamic equations (Moore, 1983):

$$Q_h = \rho_a c_{pa} D_a (T_f(t) - T_s) \quad (\text{A21})$$

and

$$Q_e = L_v D_a (\rho_f(t) - \rho_s), \quad (\text{A22})$$

where ρ_a is the density of air (kg m^{-3}), c_{pa} is the specific heat of air ($\text{J kg}^{-1} \text{°C}^{-1}$), D_a is an aerodynamic exchange coefficient (m s^{-1}), T_s is the snow surface temperature (assumed constant at 0 °C), L_v is the latent heat of vaporization (J kg^{-1}), $\rho_f(t)$ is the atmospheric vapour density under the forest canopy (kg m^{-3}), and ρ_s is the vapour density at the snow surface (kg m^{-3}), computed as the saturation value for T_s . To compute vapour densities, it was assumed that the relative humidity below the forest canopy was 100%. The transfer coefficient, D_a , was calculated using a bulk aerodynamic approach (Moore, 1983), including a stability correction based on the bulk Richardson number and an assumed roughness length of 0.025 m. A nominal wind speed of 0.8 m s^{-1} was used to compute D_a , based on measured wind speeds under forest canopy at Griffith Creek (Leach & Moore, 2014).

The sensible heat of throughfall is calculated as

$$Q_p = \rho_w c_{pw} T_f(t) (T_{tf}(t) - T_s), \quad (\text{A23})$$

where $T_{tf}(t)$ is the temperature of throughfall (°C). When snow is held in the canopy, $T_{tf}(t)$ is set to 0 °C; otherwise, it is set to the maximum of 0 °C and $T_f(t)$.

Water input to the soil is computed as the sum of $TF(t)$ and $M(t)$. If a snowpack is present, the temperature of the water input was set to 0 °C; otherwise, it was set to $T_{tf}(t)$.

A.2 | Streamflow generation description

The rate of change in water storage in the stream channel is calculated as

$$\frac{dV_c}{dt} = Q_{lat_2} + P_{cp} Lw - Q_c, \quad (\text{A24})$$

where V_c is the volume of water stored in the stream channel (m^3), Q_{lat_2} is the lateral discharge from the lower hillslope reservoir to the stream channel ($\text{m}^3 \text{s}^{-1}$) and is equivalent to the $F_{lat,2}$ term from Leach and Moore (2015), P_{cp} is channel-intercepted precipitation (m s^{-1}), L is channel reach length (m), w is mean channel width (m), and Q_c is the outflow from the catchment ($\text{m}^3 \text{s}^{-1}$), calculated as

$$Q_c = a(V_c - V_0)^b, \quad (\text{A25})$$

where a and b are parameters and V_0 is residual water storage in the channel (m^3). Parameters a and b were specified by fitting a relation between observed discharge and total channel volume calculated from the reach length, mean stream widths, and depths determined from field measurements made at Griffith Creek (Leach & Moore, 2014). The same relation was assumed to hold at East Creek considering the broad similarities in channel morphology between the two sites. The residual water storage is included in the model to account for storage in the channel (e.g., in pools) during periods when discharge from the catchment is zero (Moore et al. 2005b), and is calculated as

$$V_0 = L \cdot w \cdot \bar{d}_0, \quad (\text{A26})$$

where L is the reach length (m), w is the mean stream width during the study period (m), and \bar{d}_0 is a calibrated mean residual stream depth (m). The calibration of \bar{d}_0 is described below.

A.3 | Channel heat budget description

Stream temperature, T_w (°C), is calculated as

$$T_w = H_c / (V_c \cdot \rho_w \cdot c_{pw}), \quad (\text{A27})$$

where H_c is the heat content in the channel (J). The rate of change in H_c is calculated as

$$\frac{dH_c}{dt} = Lw(Q_* + Q_{bed} + Q_{cp}) + Q_{lat_2} \rho_w c_{pw} T_{p_2} - Q_c \rho_w c_{pw} T_w, \quad (\text{A28})$$

where L is the reach length (m), which was assumed constant; w is the stream width (m), which varied in relation to Q_c based on an empirical relationship using field measurements; Q_* , Q_{bed} , and Q_{cp} are net radiation, bed heat flux, and channel-intercepted precipitation heat flux (W m^{-2}), respectively; and T_{p_2} is the phreatic zone temperature of the lower hillslope reservoir (°C) and represents the temperature

of throughflow inputs to the stream (Leach & Moore, 2015). Considering the low wind speeds typical under preharvest conditions (Guenther et al. 2012), turbulent energy exchanges at the stream surface were assumed to be negligible and are not included in the model. Equation A28 was integrated at 6min intervals using a fourth-order Runge-Kutta scheme in the 'deSolve' package in R (Soetaert, Petzoldt, & Setzer, 2010). The 6minute values of T_w were used to calculate hourly means.

Heat flux associated with channel-intercepted precipitation, Q_{cp} (W m^{-2}), is computed as

$$Q_{cp} = \begin{cases} TF\rho_w c_{pw} T_{tf} & \text{for liquid throughfall} \\ TF_s\rho_w c_{pi} T_{tf} - TF_s\rho_w L_f & \text{for frozen throughfall,} \end{cases} \quad (\text{A29})$$

where TF and TF_s are total liquid and frozen throughfall (m s^{-1}), respectively, reaching the stream surface, T_{tf} is the temperature of throughfall ($^{\circ}\text{C}$), and c_{pi} is the specific heat of ice ($\text{J kg}^{-1} ^{\circ}\text{C}^{-1}$).

Hourly net radiation at the stream surface is computed as

$$Q_* = (1 - \alpha)K \downarrow + \epsilon_f\sigma(T_f + 273.2)^4 - \epsilon_w\sigma(T_w + 273.2)^4, \quad (\text{A30})$$

where α is the stream albedo, assumed equal to 0.05 (Oke, 1987), ϵ_f and ϵ_w are the emissivities of the forest canopy and stream surface, respectively, and T_f and T_w are the air temperature below the forest canopy and stream temperature ($^{\circ}\text{C}$), respectively. The emissivities are set at 0.95 and 0.97 for the forest canopy and stream surface, respectively (Oke, 1987).

Heat transfer from the bed to stream per unit area of channel (Q_{bed}) is computed as

$$Q_{bed} = k_{bed} \cdot (T_{bed} - T_w), \quad (\text{A31})$$

where k_{bed} is the effective stream bed transfer ($\text{W m}^{-2} \text{K}^{-1}$), which is calibrated and T_{bed} is the effective bed temperature ($^{\circ}\text{C}$) computed as

$$T_{bed} = H_{bed}/\rho_{bed} \cdot c_{p,bed} \cdot A_{bed}, \quad (\text{A32})$$

where H_{bed} is the bed heat storage (J), ρ_{bed} is the density of the bed (representing the density of saturated sediments, kg m^{-3}), $c_{p,bed}$ is the specific heat of the bed ($\text{J kg}^{-1} ^{\circ}\text{C}^{-1}$), A_{bed} is the cross-sectional area of the bed engaged in storing heat (m^2). The depth used to calculate A_{bed} is 0.5 m, which reflects typical depths of bed sediment overlaying bedrock at Griffith Creek (Guenther et al. 2014). Density of the bed (ρ_{bed}) is calculated as

$$\rho_{bed} = \phi_{bed}\rho_w + (1 - \phi_{bed}) \cdot \rho_m, \quad (\text{A33})$$

where ϕ_{bed} is the porosity of the stream bed and is assumed to be 0.3 which is typical for gravels (Freeze & Cherry, 1979), and ρ_m is the mineral particle density and is assumed to be $2,650 \text{ kg m}^{-3}$ (Campbell & Norman, 1998).

The bulk specific heat of the stream bed, $c_{p,bed}$, is calculated as

$$c_{p,bed} = \phi_{bed}c_{pw} + (1 - \phi_{bed}) \cdot c_{pm}, \quad (\text{A34})$$

where c_{pm} is the specific heat of mineral particles and is assumed to be $870 \text{ J kg}^{-1} ^{\circ}\text{C}^{-1}$ (Campbell & Norman, 1998).

The rate of change in H_{bed} is calculated as

$$dH_{bed}/dt = -Q_{bed} \quad (\text{A35})$$